

# One-quasiparticle states in $^{163, 165}\text{Ho}$ observed in the $(^3\text{He}, d)$ and $(\alpha, t)$ reactions\*

D. A. Lewis,<sup>†</sup> A. S. Broad,<sup>‡</sup> and W. S. Gray

*Cyclotron Laboratory, Physics Department, The University of Michigan, Ann Arbor, Michigan 48105*

(Received 19 August 1974)

The  $(^3\text{He}, d)$  and  $(\alpha, t)$  stripping reactions on  $^{162}\text{Dy}$  and  $^{164}\text{Dy}$  have been studied at bombarding energies of 46.5 and 45.5 MeV, respectively. Angular distributions for the  $(^3\text{He}, d)$  reaction were measured over the angular range  $0-35^\circ$ . The experimental resolution of approximately 15 keV full width at half-maximum was sufficient to permit extraction of  $l$  transfers and spectroscopic factors for 32 levels in  $^{163}\text{Ho}$  and  $^{165}\text{Ho}$  below 1.6 MeV of excitation, using the conventional distorted-wave Born approximation (DWBA). Previous identification from decay studies of the  $\frac{7}{2}^-$ [523],  $\frac{1}{2}^+$ [411], and  $\frac{3}{2}^+$ [411] bands in both nuclei, and the  $\frac{1}{2}^-$ [541] band in  $^{163}\text{Ho}$ , were confirmed. New assignments include the  $\frac{5}{2}^+$ [402] and  $\frac{9}{2}^-$ [514] bands in  $^{163}\text{Ho}$  and the  $\frac{1}{2}^-$ [541] and  $\frac{1}{2}^+$ [660] bands in  $^{165}\text{Ho}$ . Also the  $K = \frac{5}{2}$  band beginning at 1056 keV in  $^{165}\text{Ho}$  has been identified as the  $\frac{5}{2}^+$ [402] band, in contradiction to a tentative previous assignment from decay work. A few additional levels were observed which could not be positively identified with predicted Nilsson-model states. These include a level populated by  $l = 0$  transfer and another with  $l = 2$  in each isotope, in the 1.1–1.6-MeV excitation region. The presence of these transitions and their spectroscopic factors suggest fragmentation of the  $\frac{1}{2}^+$ [400] and possibly the  $\frac{3}{2}^+$ [402] orbitals. The measured elastic scattering is adequately represented by coupled-channels calculations, but not optical model predictions, when potential parameters derived from the lead region are used. With these parameters the DWBA yields spectroscopic factors which are in qualitative agreement with Nilsson-model predictions, although the over-all pattern of agreement is somewhat improved if the absolute values are reduced by 30–40%. The measured angular distributions are generally well reproduced by the DWBA except for the transition to the  $\frac{5}{2}^-$  member of the  $\frac{1}{2}^-$ [541] band in both nuclei. No other indications of possible indirect contributions to the reactions, which have been observed in neutron-transfer reactions at lower energies, were apparent in comparison with DWBA predictions.

NUCLEAR REACTIONS  $^{162, 164}\text{Dy}(^3\text{He}, d)$ ,  $E = 46.5$  MeV; measured  $\sigma(E_d, \theta)$ ,  $\theta = 0-35^\circ$ ,  $\Delta\theta = 2.5^\circ$ .  $^{162, 164}\text{Dy}(\alpha, t)$ ,  $E = 45.5$  MeV, measured  $E_d$ .  $^{163, 165}\text{Ho}$  deduced levels,  $l$ ,  $J$ ,  $\pi$ ,  $S$ . Enriched targets, DWBA analysis, resolution 15 keV, magnetic spectrograph.  $^{162}\text{Dy}(^3\text{He}, ^3\text{He})$ ,  $E = 46.5$  MeV, measured  $\sigma(E_{\text{He}}, \theta)$ .  $^{166}\text{Er}(d, d)$ ,  $E = 34.5$  MeV, measured  $\sigma(E_d, \theta)$ . Enriched targets, coupled-channel analysis.

## I. INTRODUCTION

Over the past few years a number of studies of odd- $Z$  even- $N$  rare-earth nuclei by  $(\alpha, t)$  and  $(^3\text{He}, d)$  stripping reactions have been reported.<sup>1</sup> These reactions excite the simplest modes of excitation in deformed nuclei, the one-quasiparticle states. In addition to providing verification of the Nilsson model, quantitative information regarding these states provides a basis for describing the more complicated excitations which occur in deformed nuclei, for example the states which arise from quasiparticle-phonon mixing, or the two-quasiparticle spectra of the neighboring odd-odd nuclei.

The general picture which has emerged from these studies is that spectroscopic information obtained with the aid of the distorted-wave Born approximation (DWBA) usually agrees fairly well

with the predictions of the Nilsson model when pairing is taken into account. On the other hand, several recent studies of neutron-transfer reactions<sup>2</sup> have indicated that indirect processes induced by inelastic scattering, which are ignored by the conventional DWBA, can lead to sizable changes in the magnitudes, and in some cases the shapes, of the observed angular distributions. These changes serve to modify, but usually not destroy, the over-all distribution of spectroscopic strengths within a band which would be inferred if the reaction is analyzed using the DWBA. The importance of indirect effects has not yet been investigated for the proton-transfer reactions  $(^3\text{He}, d)$  and  $(\alpha, t)$ , which have mostly been studied at bombarding energies close to the Coulomb barrier. At these energies (25–30 MeV) the angular distributions, in cases in which they have been measured, agree fairly well with DWBA

predictions but show little structure.

We present here data for the stripping reactions  $^{162,164}\text{Dy}(^3\text{He}, d)$  ( $E_{\text{He}} = 46.5$  MeV) and  $^{162,164}\text{Dy}(\alpha, t)$  ( $E_{\alpha} = 45.5$  MeV) leading to levels in  $^{163}\text{Ho}$  and  $^{165}\text{Ho}$ . In this bombarding energy range the  $(^3\text{He}, d)$  angular distributions exhibit rapid oscillations, permitting unambiguous determination of  $l$  transfers. This pronounced structure, in addition to facilitating the extraction of spectroscopic information, provides a more stringent basis for comparison with DWBA predictions than is possible at the lower energies, and thus may be useful in assessing the importance of indirect contributions to the reaction.

In the present paper the spectroscopy of  $^{163}\text{Ho}$  and  $^{165}\text{Ho}$  is discussed in the context of the conventional DWBA model. A more detailed analysis of the reaction data, in which multistep processes and form factor effects are considered, will appear in a subsequent paper.

## II. EXPERIMENTAL MEASUREMENTS

Angular distributions for the  $(^3\text{He}, d)$  reactions on  $^{162}\text{Dy}$  and  $^{164}\text{Dy}$  were measured over the angular range  $0-35^\circ$ . The measurements were made using 46.5-MeV  $^3\text{He}$  beams accelerated with The University of Michigan 83-inch cyclotron. The extracted beams were momentum analyzed by two  $135^\circ$  beam-preparation magnets to provide a 6-mm wide spot at the target. Forward-angle data were taken with the defining slits in the scattering chamber removed. In this case energy selection was accomplished by a slit placed at an intermediate image between the beam-preparation magnets. The outgoing deuterons were detected in Ilford K2 emulsions, 100  $\mu\text{m}$  thick, placed at the image surface of the second magnet of the three-stage magnetic analysis system. These exposures covered approximately the first 1.6 MeV of excitation in both  $^{163}\text{Ho}$  and  $^{165}\text{Ho}$ .

Several spectra for the  $^{162}\text{Dy}(\alpha, t)^{163}\text{Ho}$  and  $^{164}\text{Dy}(\alpha, t)^{165}\text{Ho}$  reactions were also measured in a similar way, at  $E_{\alpha} = 45.5$  MeV. The  $(\alpha, t)$  exposures were useful in picking out levels with relatively high spin, since the momentum matching conditions for this reaction favor the higher  $l$  transfers. Although the  $(\alpha, t)$  angular distributions do not have enough structure to permit reliable determination of  $l$  transfers, comparison of  $(^3\text{He}, d)$  and  $(\alpha, t)$  intensities to the same level can be used to obtain a rough measure of the probable  $l$  transfer.

The targets were produced by vacuum evaporation of isotopically enriched  $\text{Dy}_2\text{O}_3$  onto 40- $\mu\text{g}/\text{cm}^2$  carbon foils. The oxides were bombarded with 2-kV electrons which were focused to a

0.15-cm diam spot by a magnetic field. The evaporated material condensed onto the carbon foils which were placed 6 cm above the oxide pellet. After a cooling down period, the foils were floated off supporting glass slides and picked up onto target frames. Targets produced by this method usually contained 75–125  $\mu\text{g}/\text{cm}^2$  of dysprosium.

Considerable effort was made to maximize count rate while maintaining adequate resolution. Although the magnetic analysis system used with the cyclotron is capable of resolutions  $E/\Delta E$  of up to  $8 \times 10^3$  (5 keV at 40 MeV), there are several additional effects which must be considered in minimizing peak widths. One of the most important of these, for the reactions of interest here, is the scattering from atomic electrons in the target material, which determines the energy straggling of the incident and outgoing particles and the difference in their stopping powers. Since the contributions to the line width from energy loss and ion optics are both determined in part by the orientation of the target, the target angle is an important parameter. The kinematic broadening due to the convergence angle of the beam at the target is an additional consideration (kinematic broadening due to the finite aperture of the spectrometer can be compensated by adjusting the position of the image surface). Using the root mean square deviation to characterize the resolution, a computer code was written to search on the various parameters (slit sizes, target angle, *etc.*) in order to maximize count rate for a given resolution. The predicted rms deviation associated with each effect is listed in Table I for a typical spectrum from the  $^{164}\text{Dy}(^3\text{He}, d)^{165}\text{Ho}$  reaction. The target consisted of 100  $\mu\text{g}/\text{cm}^2$   $\text{Dy}_2\text{O}_3$  on a 40- $\mu\text{g}/\text{cm}^2$  carbon backing. The ion optics contribution was calculated using a source width of 2-mm with 3-mm slits placed between the two beam-preparation magnets. Although this results in an energy width of more than 35 keV on the target, the dispersion cancellation properties of the spectrometer reduce this to a tolerable level. The

TABLE I.  $20^\circ$   $^{164}\text{Dy}(^3\text{He}, d)^{165}\text{Ho}$  spectrum.

|   | rms deviation<br>(keV) |
|---|------------------------|
| Effect of electrons in target material          | 4.6                    |
| Energy straggling in target backing             | 1.9                    |
| Kinematic broadening due to beam<br>convergence | 3.8                    |
| Effect of ion optics                            | 3.2                    |
| Predicted total deviation                       | 7.0                    |
| Measured total deviation                        | 7.4                    |

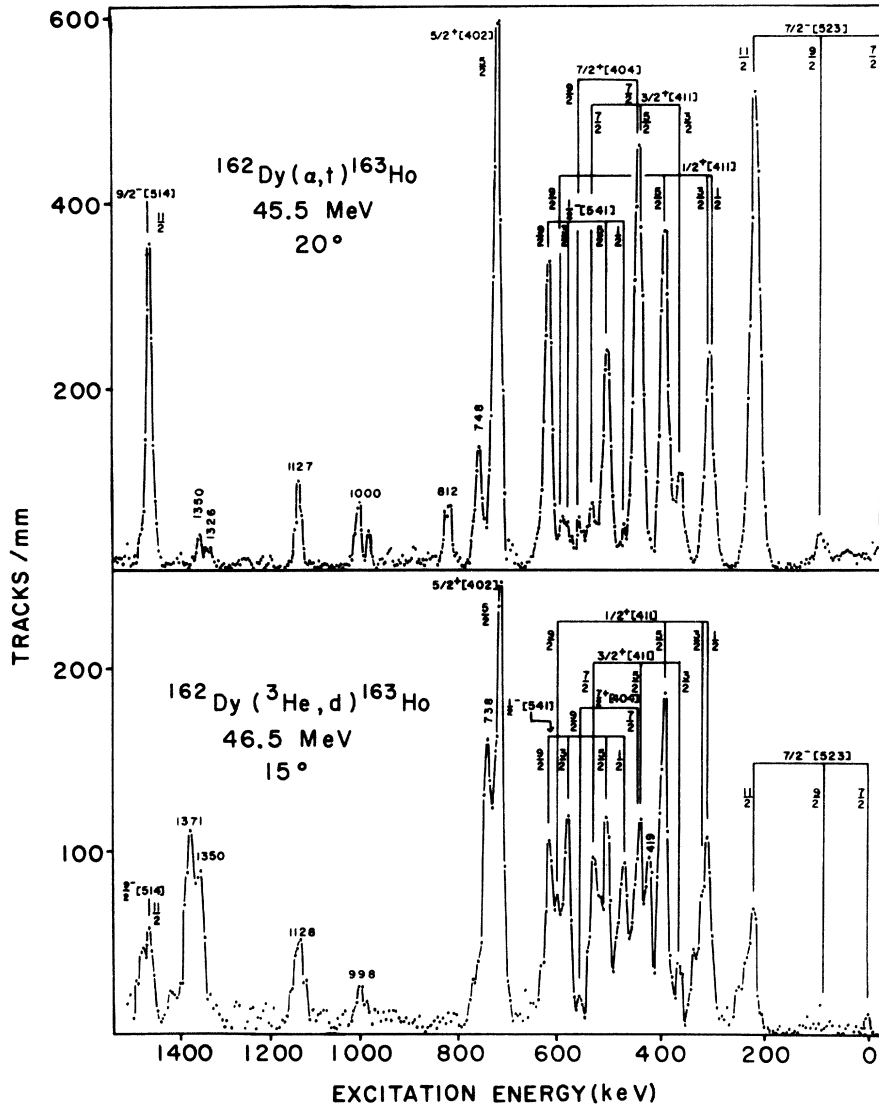


FIG. 1. Sample spectra from the  $^{162}\text{Dy}({}^3\text{He}, d){}^{165}\text{Ho}$  and  $^{162}\text{Dy}(\alpha, t){}^{163}\text{Ho}$  reactions.

convergence angle of the beam was  $1.6^\circ$ .

The difference between the predicted and measured rms deviations most likely is due to magnet aberrations and magnet regulation instabilities which were not included in the calculation. If the peak shape were Gaussian, an rms deviation of 7.4 keV would correspond to a full width at half-maximum (FWHM) of 17.5 keV. The actual peak shape is slightly narrower (15–16 keV) with a small tail due to the asymmetry of the straggling contributions.

Sample spectra for the reactions are shown in Figs. 1 and 2. The solid lines in the  $^{165}\text{Ho}$  spectra are best-fit peaks generated by the computer code AUTOFIT,<sup>3</sup> which was used to unfold unresolved levels.

As an aid to the analysis of the  $({}^3\text{He}, d)$  reactions,

cross sections for elastic and inelastic scattering of  ${}^3\text{He} + {}^{162}\text{Dy}$  were measured at 46.5 MeV. Experimental limitations precluded the measurement of deuteron scattering at the energy corresponding to the exit channel (approximately 45 MeV). Instead the deuteron scattering was measured for  $^{166}\text{Er}$  at  $E_d = 34.5$  MeV. The scattered particles were detected on a position-sensitive detector with an active length of 50 mm, which was placed at the image surface of the spectrometer. The cross sections for elastic scattering and excitation of the  $2^+$  member of the ground state rotational band were measured simultaneously with the same detector. Excitation of the  $4^+$  or higher members of the band was not measured.

The absolute normalization of the  $^{162,164}\text{Dy}({}^3\text{He}, d){}^{163,165}\text{Ho}$  and  $^{162}\text{Dy}({}^3\text{He}, {}^3\text{He})$  cross sections

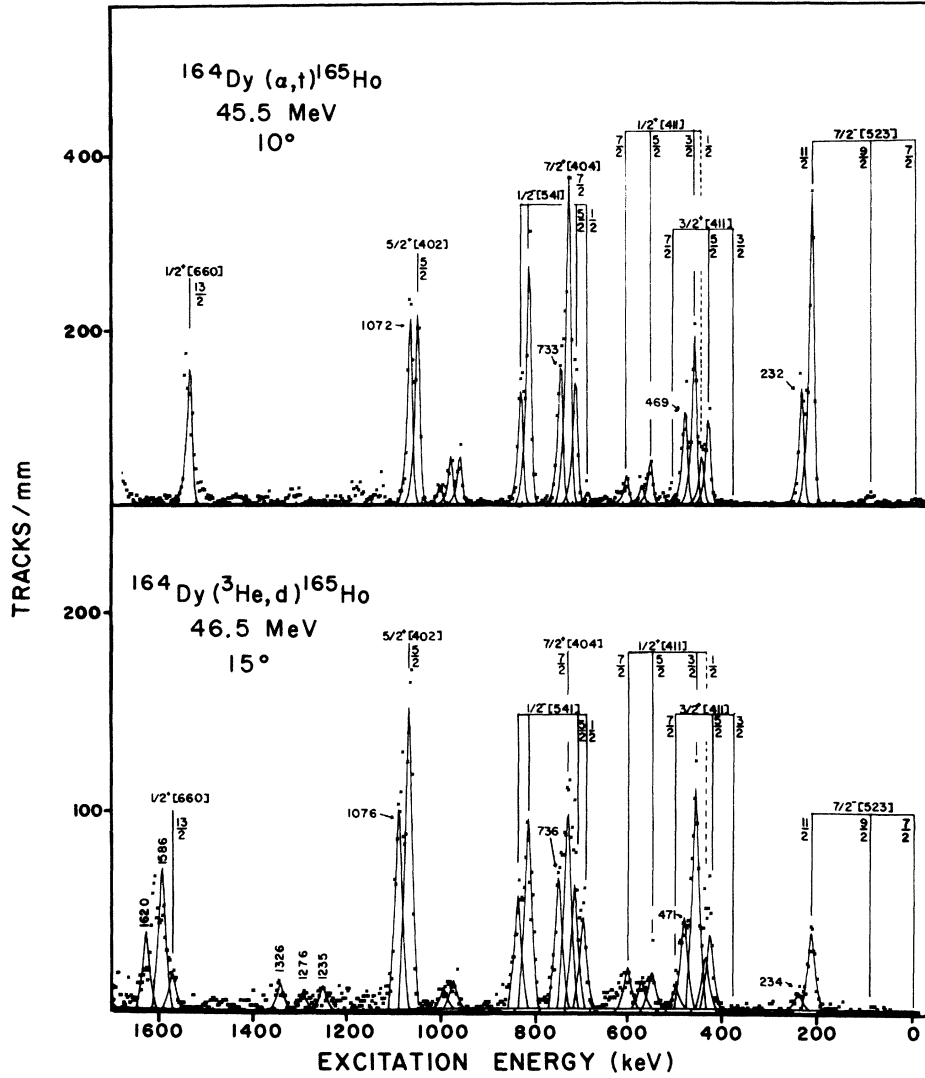


FIG. 2. Sample spectra from the  $^{164}\text{Dy}(^3\text{He}, d)^{165}\text{Ho}$  and  $^{164}\text{Dy}(\alpha, t)^{165}\text{Ho}$  reactions. The solid lines are best-fit peaks generated by the peak-fitting program AUTOFIT.

was determined by measuring the  $^3\text{He}$  elastic scattering yields at  $\pm 10^\circ$  and assuming that at this angle the elastic scattering is reproduced correctly by the optical model predictions. The  $^{166}\text{Er}(d, d)$  normalization was determined similarly. At  $10^\circ$  the deviation from purely Rutherford

scattering predicted by the optical potentials of Table II was for each projectile less than 7%. No attempt was made to normalize the  $(\alpha, t)$  cross sections, as only relative  $(^3\text{He}, d)$  and  $(\alpha, t)$  intensities were used in the analysis. Individual spectra were normalized to each other in terms

TABLE II. Potential parameters used in the DWBA analysis of the  $(^3\text{He}, d)$  reaction.

| Particle      | $V_0$<br>(MeV) | $r_0$<br>(fm) | $a$<br>(fm) | $W$<br>(MeV) | $W_D$<br>(MeV) | $r'_0$<br>(fm) | $a'$<br>(fm) | $r_c$<br>(fm) | $V_{so}$<br>(MeV) |
|---------------|----------------|---------------|-------------|--------------|----------------|----------------|--------------|---------------|-------------------|
| $d$           | 91             | 1.16          | 0.83        | 0            | 14.25          | 1.25           | 0.90         | 1.3           | 0                 |
| $^3\text{He}$ | 175            | 1.14          | 0.723       | 17.5         | 0              | 1.60           | 0.90         | 1.4           | 0                 |
| $p$           | $a$            | 1.25          | 0.63        |              |                |                |              | 1.25          | $\lambda = 15^b$  |

<sup>a</sup> Adjusted to reproduce the separation energy.

<sup>b</sup> Spin-orbit coupling  $\lambda$  times the Thomas term.

of elastic scattering yields recorded in a solid-state detector mounted at  $35^\circ$  in the scattering chamber. This technique eliminated uncertainties in target thickness due to deterioration and changes in orientation angle. The target orientation was changed with scattering angle to take advantage of the dispersion cancellation properties of the magnetic-analysis system.

The largest uncertainty in the ( $^3\text{He}, d$ ) cross sections for most levels was due to the necessity of unfolding unresolved peaks. Because of the small average level spacing ( $\sim 25$  keV) and an average experimental resolution of approximately 15 keV FWHM, very few states were clearly resolved as can be seen in Figs. 1 and 2. The spectra were analyzed using the computer code AUTOFIT. The errors assessed for the ( $^3\text{He}, d$ ) yields include estimated uncertainties in the peak-fitting procedure.

Excitation energies for known states in  $^{163}\text{Ho}$  and  $^{165}\text{Ho}$  were taken from decay studies.<sup>4,5</sup> The energies of other states were obtained relative to these using the calculated momentum dispersion of the spectrograph. The energies quoted are estimated to be accurate to  $\pm 5$  keV, except for levels above 900 keV in  $^{163}\text{Ho}$  and 1100 keV in  $^{165}\text{Ho}$ , for which the estimated uncertainty is  $\pm 10$  keV.

### III. ANALYSIS OF THE REACTIONS

#### A. Remarks

In 1958 Satchler derived expressions for the cross sections for single nucleon transfer reactions on deformed nuclei.<sup>6</sup> Assuming a direct one-step process, he showed that each member of a rotational band would be populated with a strength proportional to the square of the corresponding angular momentum component in the wave function of the transferred particle. These wave functions are usually expanded in a spherical basis as

$$\chi_\Omega = \sum_{I_j} C_{I_j} \phi_{N I_j \Omega}, \quad (1)$$

where the expansion coefficients  $C_{I_j}$  can be calculated from the Nilsson model. For an even-even target the stripping cross section to the member of a rotational band having spin  $j$  is

$$\frac{d\sigma}{d\Omega} = 2 C_{I_j}^2 U^2 \sigma_{I_j}(\theta), \quad (2)$$

where  $U^2$  is the probability that the state is unoccupied in the target ground state, and  $\sigma_{I_j}(\theta)$  is a reduced cross section reflecting the dynamics of the reaction.

Unfortunately the assumption that the reaction proceeds via a one-step process is not well justified for highly deformed rare-earth nuclei. In

recent studies of ( $d, p$ ) and ( $p, d$ ) reactions in this region,<sup>2</sup> several authors concluded that indirect processes induced by inelastic scattering may alter the cross sections to the stronger states by 10–20% and change the cross sections for the weaker transitions by an order of magnitude. One would expect to see similar effects in single-proton transfer reactions.

Another well-known difficulty is related to the expansion in Eq. (1). The expansion coefficients  $C_{I_j}$  are usually calculated for a particle bound in a deformed harmonic oscillator well. This well generates single-particle wave functions with unrealistic tails. In the usual procedure one tries to correct this by substituting wave functions from a spherical Woods-Saxon well. The depth of the well is adjusted for each  $\phi_{N I_j \Omega}$  so that the tail of the wave function has the correct slope. However, due to the truncation in the quantum number  $N$  which is implied by this procedure, there is no assurance that the magnitude of the wave function is correct in the tail region.<sup>7,8</sup> For a surface peaked reaction like ( $^3\text{He}, d$ ), this implies that the shapes of the predicted angular distributions will probably be correct, but the magnitudes may be wrong.

Despite these caveats, the standard procedure based on Eqs. (1) and (2) has proven quite useful in locating and cataloging the intrinsic single-particle states in heavy deformed nuclei. In fact, if Eq. (2) is used to extract values of  $U^2 C_{I_j}^2$  from experimental data, these values usually agree fairly well with those predicted by the Nilsson model.

#### B. Elastic and inelastic scattering

Most ( $^3\text{He}, d$ ) experiments on rare-earth nuclei have been analyzed using the  $^3\text{He}$  parameters of Parkinson *et al.*<sup>9</sup> These are given in Table II, together with the deuteron parameter set of Hintenberger *et al.*<sup>10</sup> However, both parameter sets were derived from elastic scattering experiments in the lead region and one cannot be certain that they are appropriate for elastic scattering from strongly deformed rare-earth nuclei. In addition, the likelihood of strong coupling between the elastic channel and the low-lying rotational states of these nuclei suggests the necessity of a coupled-channels treatment of the scattering problem. Accordingly, the scattering of deuterons and  $^3\text{He}$  to both the ground state and the first excited ( $2^+$ ) state was measured for  $^{162}\text{Dy}$  and  $^{166}\text{Er}$  targets in order to investigate the applicability of these parameters to reactions in the rare-earth region.

The measured angular distributions for  $^{166}\text{Er} + d$  are shown in Fig. 3. The dashed line in the

figure is an optical model (OM) calculation using the deuteron parameters of Table II. The OM prediction has too much structure beyond  $30^\circ$  and does not decrease rapidly enough as a function of the scattering angle. It was found that a rather unreasonable set of parameters, with the real well diffuseness adjusted to a value of 1 fm, was required to reproduce the over-all slope of the experimental angular distribution, and even then the detailed agreement with experiment was not very good. Since the cross section for exciting the  $2^+$  state is comparable to the elastic scattering at angles greater than  $35^\circ$  (approximately the classical grazing angle), a coupled-channels calculation was made using the Oxford Coupled-Channels Code.<sup>11</sup> Without changes in the parameters of Table II, the coupled-channels predictions for the elastic and inelastic scattering were in good agreement with the data. In this calculation coupling to the  $2^+$  and  $4^+$  member of the ground state rotational band was included,

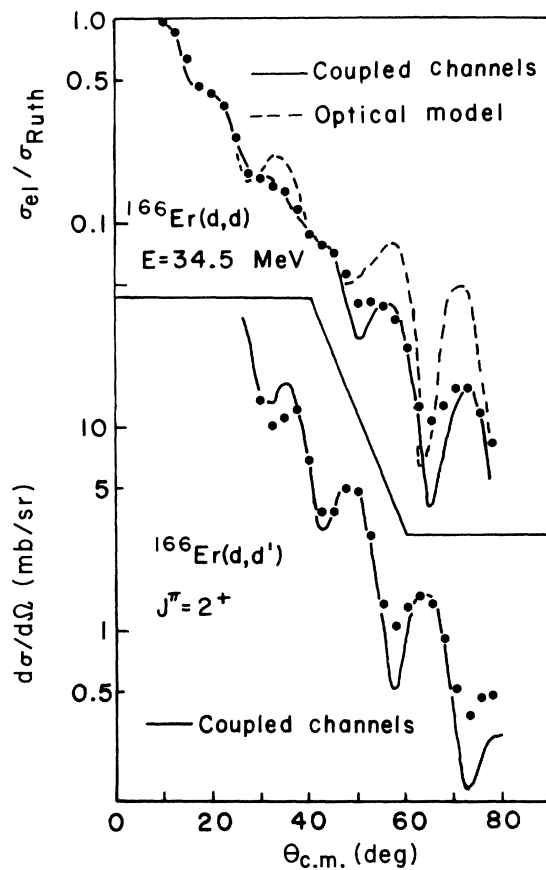


FIG. 3. Angular distributions for the elastic scattering and excitation of the first excited  $2^+$  state in  $^{166}\text{Er}$  by 34.5-MeV deuterons. The coupled-channels and optical-model predictions each use the potential set of Table II.

although excitation of the  $4^+$  state was not measured. However, since the value of  $\beta_4$  measured in other experiments<sup>12</sup> is essentially zero for nuclei near  $A = 165$ , direct hexadecapole excitation of the  $4^+$  state was not included in the coupled-channels basis. The value of  $\beta_2$  used in the calculation was 0.28, in good agreement with previous determinations of this parameter for  $^{166}\text{Er}$ .<sup>13</sup>

The measured angular distributions for  $^3\text{He}$  scattering leading to the ground state and first  $2^+$  state in  $^{162}\text{Dy}$  are shown in Fig. 4. Once again it was found that optical model parameters taken from the lead region (those of Parkinson *et al.*) were able to reproduce the elastic and inelastic scattering in a coupled-channels calculation, but that the optical model prediction was in disagreement with the elastic scattering data. However, a reasonable fit to the angular distribution for the  $2^+$  state was achieved only with a deformed Coulomb potential, a refinement which was not required to reproduce the deuteron scattering. The necessity for a Coulomb excitation term in reproducing the inelastic scattering of doubly charged particles on heavy nuclei has been indicated by many experiments.<sup>11</sup>

In view of these results, one is faced with a dilemma in choosing the optical potentials to be

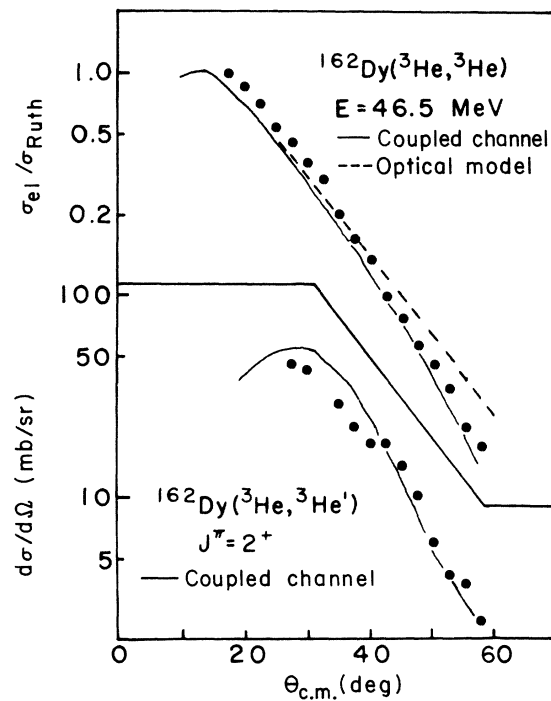


FIG. 4. Angular distributions for the elastic scattering and excitation of the first excited  $2^+$  state in  $^{162}\text{Dy}$  by 46.5-MeV  $^3\text{He}$  ions. The coupled-channels and optical-model prediction each use the potential set of Table II.

TABLE III. Comparison of experimental and predicted spectroscopic factors for bands observed in  $^{163}\text{Ho}$  and  $^{165}\text{Ho}$ . Spectroscopic factors in parentheses are rather uncertain due to large uncertainties in the measured cross sections.

| Nilsson state         | $I$            | $^{163}\text{Ho}$                      |                              |                               |                                   | $^{165}\text{Ho}$                      |                              |                               |                                   |
|-----------------------|----------------|--|------------------------------|-------------------------------|-----------------------------------|--|------------------------------|-------------------------------|-----------------------------------|
|                       |                | Experimental energy (keV) <sup>a</sup> | $U^2C_{ij}^2$ (Experimental) | $U^2C_{ij}^2$ (Nilsson model) | $U^2C_{ij}^2$ (Coriolis modified) | Experimental energy (keV) <sup>a</sup> | $U^2C_{ij}^2$ (Experimental) | $U^2C_{ij}^2$ (Nilsson model) | $U^2C_{ij}^2$ (Coriolis modified) |
| $\frac{7}{2}^-$ [523] | $\frac{7}{2}$  | 0                                      | (0.02)                       | 0.01                          | 0.01                              | 0                                      |                              | 0.01                          | 0.01                              |
|                       | $\frac{9}{2}$  | 100                                    | (0.08)                       | 0.01                          | 0.01                              | 95                                     |                              | 0.01                          | 0.01                              |
|                       | $\frac{11}{2}$ | 222                                    | 0.79                         | 0.54                          | 0.83                              | 210                                    | 0.76                         | 0.54                          | 0.83                              |
| $\frac{1}{2}^+$ [411] | $\frac{1}{2}$  | 298                                    | b                            | 0.07                          | 0.07                              | 429                                    | b                            | 0.07                          | 0.07                              |
|                       | $\frac{3}{2}$  | 308                                    | 0.55                         | 0.43                          | 0.41                              | 449                                    | 0.80                         | 0.43                          | 0.46                              |
|                       | $\frac{5}{2}$  | 392                                    | 0.90                         | 0.17                          | 0.38                              | 539                                    | 0.20                         | 0.17                          | 0.11                              |
|                       | $\frac{7}{2}$  | 431                                    |                              | 0.12                          | 0.03                              | 590                                    | 0.55                         | 0.12                          | 0.18                              |
|                       | $\frac{9}{2}$  | 588                                    | c                            | 0.02                          | 0.05                              |  |                              | 0.02                          | 0.02                              |
| $\frac{3}{2}^+$ [411] | $\frac{3}{2}$  | 360                                    | 0.20                         | 0.01                          | 0.05                              | 362                                    | <0.01                        | 0.01                          | 0.00                              |
|                       | $\frac{5}{2}$  | 441                                    | b                            | 0.24                          | 0.19                              | 420                                    | 0.52                         | 0.24                          | 0.37                              |
|                       | $\frac{7}{2}$  | 528                                    | c                            | 0.04                          | 0.07                              | 491                                    | c                            | 0.04                          | 0.03                              |
| $\frac{1}{2}^-$ [541] | $\frac{1}{2}$  | 471                                    | 0.11                         | 0.04                          | 0.04                              | 681 <sup>d</sup>                       | 0.10                         | 0.04                          | 0.04                              |
|                       | $\frac{3}{2}$  | 578                                    | 0.17                         | 0.04                          | 0.04                              | 798 <sup>e</sup>                       | 0.22 ( $l=1$ )               | 0.04                          | 0.04                              |
|                       |                |  |                              |                               |                                   | 820 <sup>e</sup>                       | 0.11 ( $l=1$ )               |                               |                                   |
|                       | $\frac{5}{2}$  | 500                                    | 0.75                         | 0.20                          | 0.22                              | 702 <sup>d</sup>                       | 0.20                         | 0.20                          | 0.23                              |
|                       | $\frac{7}{2}$  |  |                              | 0.03                          | 0.04                              |  |                              | 0.03                          | 0.04                              |
| $\frac{7}{2}^+$ [404] | $\frac{7}{2}$  | 440                                    | b                            | 0.90                          | 1.08                              | 716                                    | (2.0)                        | 0.90                          | 0.99                              |
|                       | $\frac{9}{2}$  | 552                                    | (0.07)                       | 0.01                          | 0.01                              | 820                                    |                              | 0.01                          | 0.02                              |
| $\frac{5}{2}^+$ [402] | $\frac{5}{2}$  | 713 <sup>d</sup>                       | 1.40                         | 0.89                          | 0.74                              | 1056 <sup>d</sup>                      | 1.20                         | 0.89                          | 0.82                              |
| $\frac{9}{2}^-$ [514] | $\frac{9}{2}$  |  |                              | 0.01                          | 0.01                              |  |                              | 0.01                          | 0.01                              |
|                       | $\frac{11}{2}$ | 1465 <sup>d</sup>                      | 0.98                         | 0.93                          | 0.92                              |  |                              | 0.93                          | 0.92                              |
| $\frac{1}{2}^+$ [660] | $\frac{9}{2}$  |  |                              | 0.16                          |                                   |  |                              | 0.16                          |                                   |
|                       | $\frac{13}{2}$ |  |                              | 0.79                          |                                   | 1561 <sup>d</sup>                      | 0.90                         | 0.79                          |                                   |

<sup>a</sup> Excitation energies are an average of ( $^3\text{He}, d$ ) and ( $\alpha, t$ ) values, calibrated from energies measured in Refs. 4 and 5.

<sup>b</sup> Not resolved.

<sup>c</sup> A transition was observed within approximately 5 keV of the energy reported in Ref. 4 or Ref. 5, but overlapping peaks or the character of the angular distribution prevented extraction of a reliable spectroscopic factor.

<sup>d</sup> New assignment from this work.

<sup>e</sup> Both these levels have ( $^3\text{He}, d$ ) angular distribution indicative of  $l=1$ , while the ( $\alpha, t$ )/( $^3\text{He}, d$ ) yield ratios indicate  $l=4$  or 5 (see text).

used in a DWBA analysis of the stripping reaction. On the grounds of consistency, optical potentials used in a DWBA calculation should reproduce the elastic scattering. On the other hand, we see that the potential parameters of Table II are capable of reproducing both elastic and inelastic scattering when the strong coupling to inelastic channels is properly taken into account.

Some guidance in resolving this question is provided by a study of ( $d, p$ ) reactions on strongly

deformed nuclei by Siemssen and Erskine.<sup>15</sup> These authors found that when optical potentials which fit the elastic scattering were used in the DWBA calculations, the resulting spectroscopic factors generally exceeded Nilsson-model predictions by approximately a factor of 2. Use of an average set of parameters derived from spherical nuclei yielded spectroscopic factors in somewhat better agreement with expectations but, as in the present case, they failed to reproduce the elastic scat-

tering. Accordingly, we have chosen to use the optical potentials of Table II in the analysis of the  $(^3\text{He}, d)$  data.

### C. Distorted-wave analysis

The  $(^3\text{He}, d)$  data were analyzed with the DWBA code DWUCK,<sup>16</sup> using the optical parameters of Table II. All calculations employed the zero-range approximation, and corrections for nonlocality were not included. The over-all normalization factor for the  $(^3\text{He}, d)$  reaction was taken to be 4.42, in accordance with the estimate of Bassel.<sup>17</sup> The radial wave function for the transferred proton was generated in a spherical Woods-Saxon well using the usual separation-energy prescription.

A question which arises in analyzing proton-transfer reactions on heavy nuclei is whether to use a radial cutoff. In an analysis of the  $(d, ^3\text{He})$  reaction on  $^{208}\text{Pb}$  which employed the optical parameters of Table II, a cutoff of 8.8 fm was found necessary to reproduce the shapes of the measured angular distributions, although use of the cutoff had only a small effect on the magnitudes of the predicted cross sections.<sup>9</sup> On the other hand, the angular distributions measured in the present experiment are generally reproduced quite well by the DWBA without a cutoff. The need for a cutoff is also less evident for  $(^3\text{He}, d)$  reactions in the lead region for which the available data cover approximately the same angular range as that of the present experiment.<sup>9,18</sup> Consequently, no

cutoff was used in the analysis.

The  $(^3\text{He}, d)$  angular distributions were used to determine  $l$  transfers. These were generally unambiguous, except in cases for which the data were poor due to statistics or overlapping peak problems. The  $(\alpha, t)/(^3\text{He}, d)$  cross section ratios served to reinforce our assignments. After the  $l$  transfer had been determined, Eq. (2) was used to extract "experimental" values of  $U^2C_{lj}^2$  from the  $(^3\text{He}, d)$  cross sections. These are listed in columns 4 and 8 of Table III.

### IV. RESULTS AND DISCUSSION

Several bands in  $^{163}\text{Ho}$  and  $^{165}\text{Ho}$  have been identified in decay studies.<sup>4,5</sup> Our work confirms most of these assignments and adds some new ones. New assignments resulting from the present experiment include the location of the  $\frac{5}{2}^+[402]$  and  $\frac{5}{2}^- [514]$  bands in  $^{163}\text{Ho}$  and the  $\frac{1}{2}^- [541]$  and  $\frac{1}{2}^+ [660]$  bands in  $^{165}\text{Ho}$ . Also the  $K = \frac{5}{2}$  band beginning at 1056 keV in  $^{165}\text{Ho}$  has been identified as the  $\frac{5}{2}^+[402]$  band, in contradiction to a tentative assignment of  $\frac{5}{2}^- [532]$  from decay work.<sup>5</sup> In addition several levels were observed in each nucleus which could not be definitely assigned to expected Nilsson-model states. Some of these will be discussed at the end of this section.

The following paragraphs consist of remarks about various bands observed in both nuclei. The  $(^3\text{He}, d)$  angular distributions are shown in Figs.

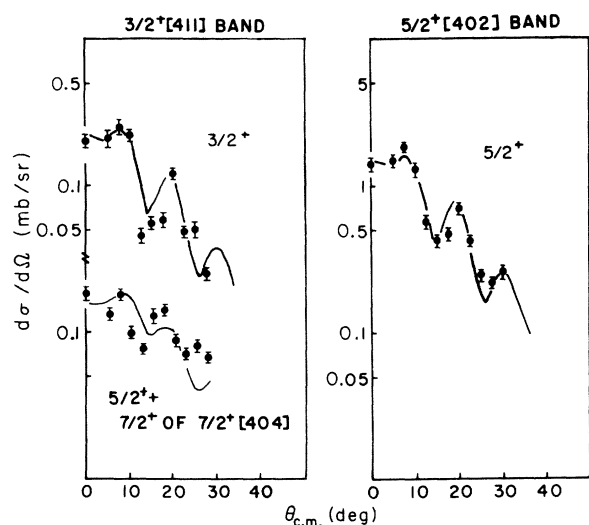


FIG. 5. Some angular distributions measured for the  $^{162}\text{Dy}(^3\text{He}, d)$  reaction. The solid curves are DWBA predictions for the  $l$  transfer indicated by the spin and parity of the final state. The DWBA curve shown with the unresolved doublet consisting of the  $\frac{5}{2}^+$  member of the  $\frac{3}{2}^+[411]$  band and the  $\frac{7}{2}^+$  [404] bandhead is a mixture of  $l=2$  and 4 (see text).

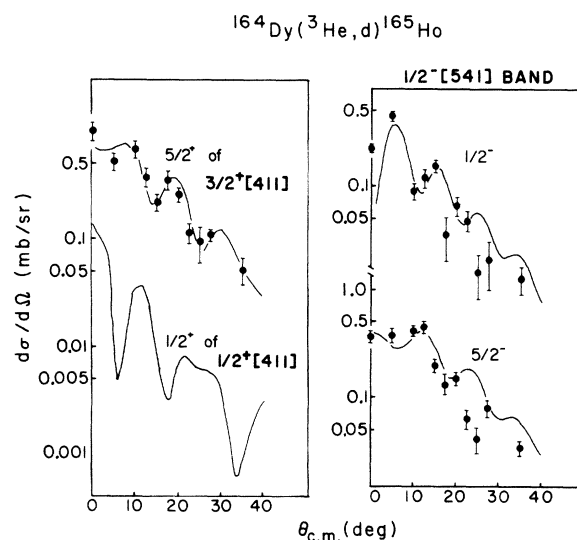


FIG. 6. Some angular distributions measured for the  $^{164}\text{Dy}(^3\text{He}, d)^{165}\text{Ho}$  reaction. The solid curves are DWBA predictions for the  $l$  transfer indicated by the spin and parity of the final state. The curve representing the bandhead of the  $\frac{1}{2}^+[411]$  band is normalized to reflect the predicted value of  $U^2C_{lj}^2$  for this level (see text).



5-11. Unless otherwise stated, all of the DWBA predictions in the figures have been normalized to fit the data and correspond to the  $l$  transfer indicated by the spin and parity of the final state.

$\frac{7}{2}^-$  [523] band

The ground state band originates in the  $h_{11/2}$  subshell, and almost all of its spectroscopic strength remains in the  $\frac{1}{2}^-$  member. For both nuclei the  $\frac{7}{2}^-$  and  $\frac{9}{2}^-$  peaks were comparable to the background, but rough estimates of  $U^2C_{lj}^2$  for these states in  $^{163}\text{Ho}$  are given in Table III.

$\frac{3}{2}^+$  [411] band

In both nuclei the  $\frac{3}{2}^+$  bandhead is cleanly separated from all other levels in the spectrum, but its cross section was large enough to measure only in  $^{163}\text{Ho}$ . The  $\frac{5}{2}^+$  member in  $^{163}\text{Ho}$  was not resolved from the  $\frac{7}{2}^+$  [404] bandhead. The combined angular distribution for these two levels is shown in Fig. 5. The solid curve is a combination of  $l=2$  and  $l=4$  DWBA predictions with the coefficients determined from a least-squares fit to the data ( $U^2C_{lj}^2=0.13$ ,  $l=2$ ; and  $U^2C_{lj}^2=0.38$ ,  $l=4$ ). The fit is not impressive. If the theoretically predicted spectroscopic factors are used (Table III), the agreement is worsened.

In  $^{165}\text{Ho}$  the  $\frac{5}{2}^+$  level was not resolved from the  $\frac{1}{2}^+$  [411] bandhead. The combined angular distribution is shown in Fig. 6. The  $l=0$  transition to the  $\frac{1}{2}^+$  state is predicted to be very weak in comparison. (Its theoretical cross section is also shown

in the figure.) The  $U^2C_{lj}^2$  value for the  $\frac{5}{2}^+$  state was therefore extracted ignoring the contribution from the  $\frac{1}{2}^+$  state. Small cross sections and overlapping peak problems prevented the measurement of the  $\frac{7}{2}^+$  and  $\frac{9}{2}^+$  cross sections. (A transition observed to a level or levels near the  $\frac{7}{2}^+$  member in  $^{163}\text{Ho}$  is discussed in the next section.)

$\frac{1}{2}^+$  [411] band

In  $^{163}\text{Ho}$  the  $\frac{1}{2}^+$  and  $\frac{3}{2}^+$  members of this band are only 10 keV apart<sup>4</sup> and were not resolved. The combined angular distribution is plotted in Fig. 7, together with a DWBA prediction for  $l=2$ . The cross section for the  $\frac{1}{2}^+$  state is predicted to be considerably smaller, making it possible to extract a  $U^2C_{lj}^2$  value for the  $\frac{3}{2}^+$  member. The angular distribution for the  $\frac{5}{2}^+$  state is plotted in the same figure. Overlapping peaks obscured the  $\frac{7}{2}^+$  and  $\frac{9}{2}^+$  members in this nucleus, although a weak transition which may correspond to the  $\frac{9}{2}^+$  level (reported<sup>4</sup> to be at 588 keV) was partially resolved in a few spectra. The angular distributions of the  $\frac{3}{2}^+$ ,  $\frac{5}{2}^+$ , and  $\frac{7}{2}^+$  members of the band in  $^{165}\text{Ho}$  are plotted in Fig. 8.

$\frac{1}{2}^-$  [541] band

The angular distributions for the  $\frac{1}{2}^-$  and  $\frac{5}{2}^-$  members of this band in  $^{165}\text{Ho}$  are shown in Fig. 6. The energies of the  $\frac{3}{2}^-$  and  $\frac{9}{2}^-$  members are expected to be very close after Coriolis coupling

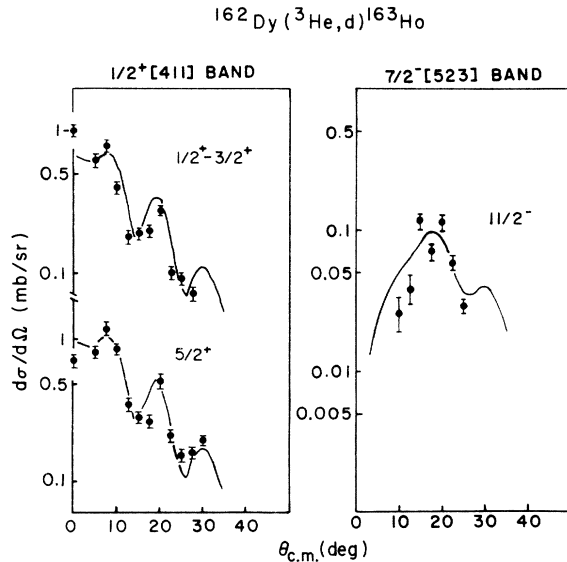


FIG. 7. Some angular distributions measured for the  $^{162}\text{Dy}(^3\text{He}, d)^{163}\text{Ho}$  reaction. The solid curves are DWBA predictions for the  $l$  transfer indicated by the spin and parity of the final state.

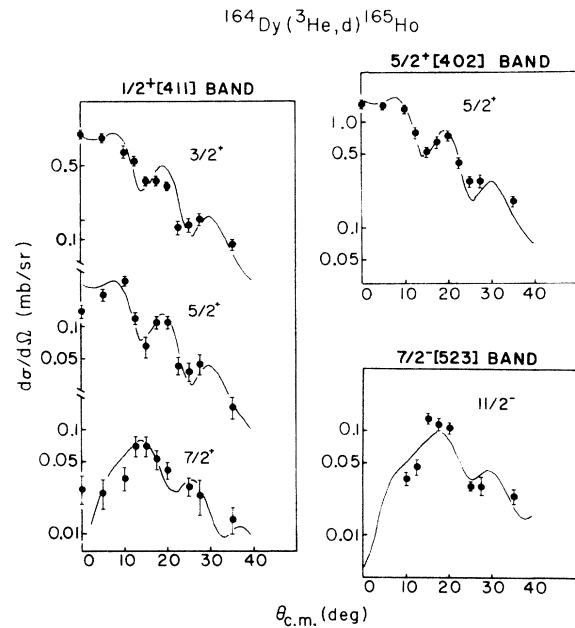


FIG. 8. Some angular distributions measured for the  $^{164}\text{Dy}(^3\text{He}, d)^{165}\text{Ho}$  reaction. The solid curves are DWBA predictions for the  $l$  transfer indicated by the spin and parity of the final state.

is taken into account. Two levels appear in the spectra at 798 and 820 keV excitation in  $^{165}\text{Ho}$  which could be these two states. However, the angular distributions for both transitions (Fig. 11) indicate that each has an  $l$  transfer of 1, whereas the  $(\alpha, t)/(^3\text{He}, d)$  cross section ratios imply that both have an  $l$  transfer of 4 or 5. The anomaly is probably due to additional unresolved states in this part of the spectrum.

Angular distributions were measured for the  $\frac{1}{2}^-$ ,  $\frac{3}{2}^-$ ,  $\frac{5}{2}^-$ , and  $\frac{9}{2}^-$  members of the band in  $^{163}\text{Ho}$ . These are shown in Fig. 9. It is interesting to note that for the  $\frac{5}{2}^-$  level in both nuclei the agreement between the measured angular distributions resemble most closely an  $l=3$  curve, but the positions of both the first and second maxima are poorly predicted by the DWBA. This is the only case appearing in the present experiment in which there is a noticeable discrepancy between experiment and the shapes of predicted DWBA angular distributions.

$\frac{7}{2}^+$  [404] band

In both nuclei this band was identified. However, overlapping peak problems made it impossible to extract spectroscopic information, except for the bandhead in  $^{165}\text{Ho}$  and the  $\frac{9}{2}^+$  member in  $^{163}\text{Ho}$ , for which rather uncertain values of  $U^2C_{lj}^2$  are given in Table III.

$\frac{5}{2}^+$  [402] band

Almost all the spectroscopic strength of this band is expected in the bandhead, which would lead to a single strong  $l=2$  transition in the stripping reactions. A level at 713 keV in  $^{163}\text{Ho}$  and another at 1056 keV in  $^{165}\text{Ho}$  both have characteristic  $l=2$  angular distributions with spectroscopic factors of approximately unity. In a decay study<sup>5</sup> the 1056-keV level in  $^{165}\text{Ho}$  was assigned a spin of  $\frac{5}{2}$  and interpreted as the  $\frac{5}{2}^-$ [532] bandhead. The stripping data conclusively contradict this interpretation and strongly suggest an alternative  $\frac{5}{2}^+$ [402] assignment for this level, as well as for the 713-keV level in  $^{163}\text{Ho}$ .

$\frac{9}{2}^-$  [514] band

In  $^{163}\text{Ho}$  a strong transition, indicative of a high  $l$  transfer, appears at 1470 keV in the  $(\alpha, t)$  reaction. In the  $(^3\text{He}, d)$  spectra a peak is observed at 1460 keV which, although appearing to be a doublet at a few angles (see Fig. 1), has an angular distribution characteristic of  $l=5$  with  $U^2C_{lj}^2$  near unity. Since the discrepancy (10 keV) between the energies measured in the two reactions is comparable to the estimated uncertainty

of excitation energies determined from this portion of the spectrum, we assume that the same level is excited in both reactions. The nearest Nilsson orbitals which might lead to a strong  $l=5$  transition are the  $\frac{9}{2}^-$ [514] and the  $\frac{3}{2}^-$ [532] states, which are predicted to have almost all of their strength in the  $\frac{1}{2}^-$  and  $\frac{9}{2}^-$  members, respectively. On the basis of energies, the most likely of the two possibilities is the  $\frac{9}{2}^-$ [514], which is expected at about this energy while the  $\frac{3}{2}^-$ [532] is predicted to be roughly 1 MeV higher. However, an additional consideration is the presence of a level at 1371 keV for which the angular distribution is characteristic of  $l=3$ . Although the spacing between the 1371- and 1460-keV levels is approximately that expected between the  $\frac{7}{2}^-$  and  $\frac{9}{2}^-$  members of the  $\frac{3}{2}^-$ [532] band, the calculations described later in this section predict an undetectably small spectroscopic factor ( $U^2C_{lj}^2 < 0.01$ ) for the  $\frac{3}{2}^-$ ,  $\frac{5}{2}^-$ , and  $\frac{7}{2}^-$  members of this band, while for the 1371-keV level we obtain  $U^2C_{lj}^2 = 0.29$ . Thus, we conclude that the 1371-keV level is unlikely to arise from the  $\frac{3}{2}^-$ [532] band and, primarily on the basis of energetics, interpret the 1460-keV level as the  $\frac{1}{2}^-$  member of the  $\frac{9}{2}^-$ [514] band. This band was not identified in  $^{165}\text{Ho}$ .

$\frac{1}{2}^+$  [660] band

In  $^{165}\text{Ho}$  a level appears at 1561 keV for which the  $(\alpha, t)/(^3\text{He}, d)$  yield ratio suggests  $l \sim 5$  or 6 and the  $(^3\text{He}, d)$  angular distribution (Fig. 11)

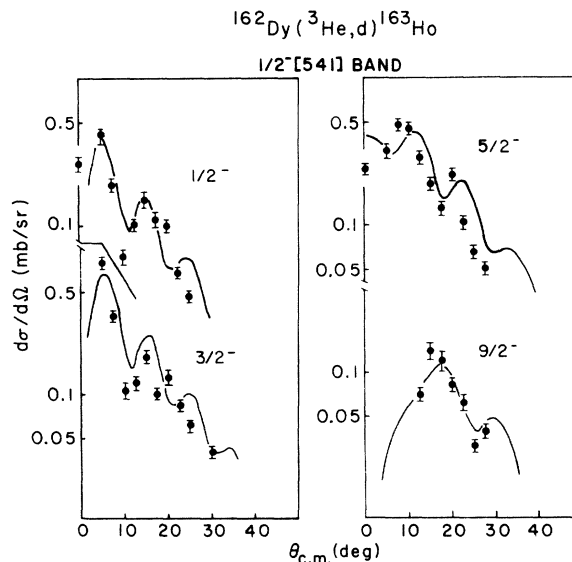


FIG. 9. Some angular distributions measured for the  $^{162}\text{Dy}(^3\text{He}, d)^{163}\text{Ho}$  reaction. The solid curves are DWBA predictions for the  $l$  transfer indicated by the spin and parity of the final state.

indicates  $l=6$  with  $U^2C_{ij}^2=0.9$ . As a basis for judging the confidence level of this assignment, the prediction for  $l=5$  is also shown in the figure. Although these two  $l$  transfers resemble one another more closely than other pairs differing by one unit, the decided preference for  $l=6$  seems to justify a definite assignment.

This strong  $l=6$  transition indicates the presence of one of the bands originating in the  $i_{13/2}$  shell model state, the lowest of which is expected to be  $\frac{1}{2}^+[660]$ . Because of the large positive decoupling parameter ( $a \sim 6.5$ ) predicted<sup>19</sup> for this band, the  $\frac{1}{2}^+$  and  $\frac{3}{2}^+$  members are expected at approximately the same energy. Very close to the 1561-keV level a transition with  $l=0$  and  $U^2C_{ij}^2 \sim 0.3$  is observed to a level at 1586 keV. However, the measured  $l=0$  strength is much greater than would be expected for the  $\frac{1}{2}^+[660]$ , since almost all the spectroscopic strength is expected to appear in the  $\frac{1}{2}^+$  member. For this and other reasons to be discussed later, we conclude that while the 1561-keV level is most likely the  $\frac{1}{2}^+$  member of the  $\frac{1}{2}^+[660]$  band, the  $\frac{1}{2}^+$  level at 1586 keV is probably of another nature.

#### $\gamma$ vibrations

None of the experimentally known  $\gamma$  vibrations were observed in this study. The  $K-2$   $\gamma$  vibration built on the ground state band has been previously identified in  $^{163}\text{Ho}$  at 560 keV<sup>20</sup> and in  $^{165}\text{Ho}$  at 514 keV.<sup>21</sup> According to Soloviev and Vogel<sup>22</sup> it has a small one-quasiparticle component due to mixing with the  $\frac{3}{2}^-[541]$  band. Since the Nilsson model predicts that the  $\frac{3}{2}^-[541]$  band occurs at an energy more than 2 MeV below the ground state, one would expect to excite the  $K-2$   $\gamma$  vibration only very weakly in the stripping reactions. The  $K+2$   $\gamma$  vibration built on the ground state band has been previously identified only in  $^{165}\text{Ho}$ .<sup>21</sup> Soloviev and Vogel predict that the single quasiparticle admixture in this state is about 0.1%. This is consistent with the fact that it was not observed.

#### Other levels

In addition to levels which could be assigned with some confidence to known or expected Nilsson-model states, several others were observed in  $^{163}\text{Ho}$  and  $^{165}\text{Ho}$  for which assignments are either tentative or were not possible. The information obtained regarding these levels is given in Table IV. For most of them definitive angular distributions could not be obtained either because of low yields or overlapping peaks, although in some cases it was possible to obtain a rough estimate of the  $l$  transfer by comparing  $(\alpha, t)$  and  $(^3\text{He}, d)$

TABLE IV. Additional levels observed but not assigned to Nilsson states. When a single  $l$  transfer and a spectroscopic factor are given, these were obtained from the  $(^3\text{He}, d)$  angular distribution.

| $E_x$ ( $^3\text{He}, d$ )<br>(keV) | $E_x$ ( $\alpha, t$ )<br>(keV) | $l$        | $U^2C_{ij}^2$  |
|-------------------------------------|--------------------------------|------------|----------------|
| $^{163}\text{Ho}$                   |                                |            |                |
| 419                                 |                                |            |                |
| 527                                 | 528                            | $\leq 2^a$ |                |
| 594                                 |                                |            |                |
| 738                                 | 748                            | $\leq 2^a$ |                |
|                                     | 812                            | $\geq 5^a$ |                |
| 998                                 | 1000                           |            |                |
| 1128                                | 1127                           | 2          | 0.20           |
|                                     | 1326                           |            |                |
| 1350                                | 1347                           | 0          | 0.30           |
| 1371                                |                                | 3          | 0.29           |
| $^{165}\text{Ho}$                   |                                |            |                |
| 234                                 | 232                            | 5          | 0.30           |
| 471                                 | 469                            | $2-3^a$    |                |
| 736                                 | 733                            | $3-4^a$    |                |
| 1076                                | 1072                           | $2-3^a$    | 0.92 ( $l=3$ ) |
| 1235                                |                                |            |                |
| 1276                                |                                |            |                |
| 1326                                |                                | 2          | 0.15           |
| 1375                                |                                |            |                |
| 1586                                |                                | 0          | 0.33           |
| 1620                                |                                | $\leq 2^a$ |                |

<sup>a</sup> Estimated range of probable  $l$  transfer inferred from  $(\alpha, t)/(^3\text{He}, d)$  yield ratios (see text).

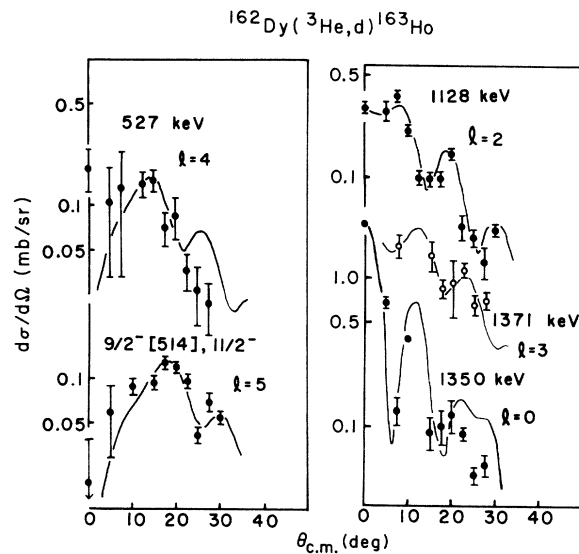


FIG. 10. Some angular distributions measured for the  $^{162}\text{Dy}(^3\text{He}, d)^{163}\text{Ho}$  reaction. The solid curves are DWBA predictions for the  $l$  transfers indicated in the figure.

yields. However, in a few cases the  $(^3\text{He}, d)$  angular distributions were sufficiently unambiguous to permit determination of the  $l$  transfer and spectroscopic factor. These angular distributions are shown in Figs. 10 and 11.

It should be mentioned that in contrast to the lower-energy experiments listed in Ref. 1, estimates of  $l$  transfers based solely on  $(\alpha, t)/(^3\text{He}, d)$  yield ratios are expected to be somewhat less reliable owing to the increased structure of the  $(^3\text{He}, d)$  angular distributions. The range of possible  $l$  transfers given for some levels in Table IV indicates that the measured yield ratio falls well within the range of values measured for other levels with these  $l$  transfers, determined from the  $(^3\text{He}, d)$  angular distributions.

In  $^{163}\text{Ho}$  a level observed at 527 keV lies very close to the previously assigned  $\frac{7}{2}^+$  member of the  $\frac{3}{2}^+[411]$  band at 528 keV. However, the agreement between the experimental angular distribution and the  $l=4$  DWBA prediction (Fig. 10) is not very convincing, and the ratio of  $(\alpha, t)/(^3\text{He}, d)$  yields suggests  $l \leq 2$  for this level. Moreover, the value of  $U^2C_{lj}^2$  which would be obtained assuming that this is the  $\frac{7}{2}^+$  level is approximately unity, a much higher value than predicted (see Table III). It seems likely that two or more unresolved levels are present at about this energy.

The most puzzling of the unidentified levels observed in  $^{165}\text{Ho}$  is at 234 keV, which based upon the  $(^3\text{He}, d)$  angular distribution (Fig. 10) and  $(\alpha, t)/(^3\text{He}, d)$  yield ratios is populated by

$l=5$  transfer with  $U^2C_{lj}^2=0.3$ . This level was not observed in previous decay studies, and the Nilsson model offers no suitable candidate for so strong an  $l=5$  transition at this excitation energy. Nevertheless, it seems highly unlikely that the transition arises from a target impurity. The corresponding peak appears with the same intensity, relative to the nearby  $\frac{1}{2}^-$  member of the  $\frac{7}{2}^-[523]$  band, in both  $(^3\text{He}, d)$  and  $(\alpha, t)$  spectra taken with three different targets made from different samples of enriched  $^{164}\text{Dy}$ . In addition reaction kinematics and ground state  $Q$  values rule out all but a few neighboring rare-earth isotopes as possible sources of the observed transition.

A fairly strong transition observed at 1076 keV in  $^{165}\text{Ho}$  is very close to the position of the  $\frac{7}{2}^+$  member of the  $\frac{5}{2}^+[413]$  band, which has been identified in decay work.<sup>5</sup> There are also indications in the  $(^3\text{He}, d)$  and  $(\alpha, t)$  spectra of two or three very weak transitions near the reported energy of the  $\frac{5}{2}^+$  bandhead. The strength of this band is predicted to be mainly in the  $\frac{7}{2}^+$  member, but the  $\frac{5}{2}^+[413]$  state is expected to be well below the Fermi surface and even the  $\frac{7}{2}^+$  level should be excited only weakly in the stripping reactions. The  $(^3\text{He}, d)$  angular distribution for the 1076-keV peak, which is shown in Fig. 10, is inconsistent with  $l=4$  and for this  $l$  transfer would yield an unreasonably large value of  $U^2C_{lj}^2$  (roughly 4) if the peak is assumed to be due solely to the  $\frac{7}{2}^+$  level. Although the angular distribution has the

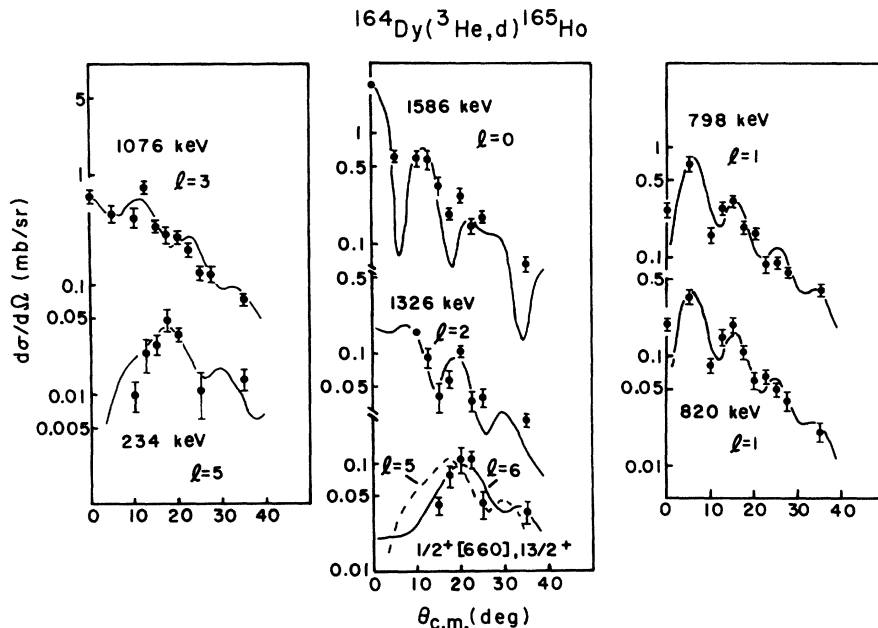


FIG. 11. Some angular distributions measured for the  $^{164}\text{Dy}(^3\text{He}, d)^{165}\text{Ho}$  reaction. The solid curves are DWBA predictions for the  $l$  transfers indicated in the figure.

same general slope as  $l=3$  prediction shown in the figure and the  $(\alpha, t)/({}^3\text{He}, d)$  yield ratio is consistent with this  $l$  transfer, the detailed agreement does not seem good enough to warrant a definite assignment. It is possible that at least two unresolved levels are present at this energy.

Above the position of the  $\frac{5}{2}^+[402]$  bandhead in both  ${}^{163}\text{Ho}$  and  ${}^{165}\text{Ho}$ , only a few strong transitions were observed up to 1.6 MeV in excitation. Of these the  $\frac{11}{2}^-, \frac{9}{2}^- [514]$  level in  ${}^{163}\text{Ho}$  and the  $\frac{13}{2}^+, \frac{1}{2}^+ [660]$  level in  ${}^{165}\text{Ho}$  have been discussed earlier. In addition, it was possible to determine  $l$  transfers for a pair of positive-parity levels in each isotope whose structure can only be tentatively determined from the available evidence.

At 1128 keV in  ${}^{163}\text{Ho}$  and 1326 keV in  ${}^{165}\text{Ho}$ , we observe a transition with  $l=2$  and  $U^2C_{ij}^2 \sim 0.2$ . Approximately 250 keV higher in each nucleus, at 1350 and 1586 keV, we find an  $l=0$  with  $U^2C_{ij}^2 \sim 0.3$ . It was pointed out in the discussion of the  $\frac{1}{2}^+[660]$  band that the 1586-keV level in  ${}^{165}\text{Ho}$  falls near the expected position of the  $\frac{1}{2}^+$  member of the band, but that the large spectroscopic factor indicates that it is of a different origin. Of the unaccounted-for Nilsson orbitals which would be expected to lead to  $l=0$  or 2 transitions strong enough to be measureable, only the  $\frac{3}{2}^+[402]$  and the  $\frac{1}{2}^+[400]$  might reasonably be expected to appear as particle states near this region of excitation. Both these bands are expected to rise in energy with increasing deformation, and at a deformation appropriate for the holmium isotopes, are predicted<sup>23</sup> to lie well above the  $\frac{1}{2}^+[660]$ . In going from  ${}^{163}\text{Ho}$  to  ${}^{165}\text{Ho}$  the center of gravity of the  $l=0$  and 2 pair shifts upward in excitation by roughly the same amount as is observed for the  $\frac{7}{2}^+[404]$  and  $\frac{3}{2}^+[402]$ , suggesting that these transitions also originate from  $N=4$  orbitals. According to Chi<sup>19</sup> the  $\frac{3}{2}^+[402]$  would have most of its spectroscopic strength in the  $\frac{3}{2}^+$  bandhead while most of the strength of the  $\frac{1}{2}^+[400]$  is expected to be divided between the  $\frac{1}{2}^+$  and  $\frac{3}{2}^+$  members, with the  $\frac{3}{2}^+$  level expected to be approximately 40–50 keV above the bandhead. The spectroscopic factor obtained for the  $l=2$  transitions in each nucleus is only 20–25% of the value expected for the  $\frac{3}{2}^+[402]$  bandhead, while the  $l=0$  transitions have only half the strength expected for the bandhead of the  $\frac{1}{2}^+[400]$ . Also no obvious candidate for a  $\frac{3}{2}^+$  member of the  $\frac{1}{2}^+[400]$  is found at the right energy relative to the  $l=0$  transitions, except for a level at 1620 keV in  ${}^{165}\text{Ho}$  for which we estimate  $l \leq 2$  from  $(\alpha, t)/({}^3\text{He}, d)$  yield ratios but could not obtain a reliable  $l$  transfer from the  $({}^3\text{He}, d)$  angular distribution. Thus it is clear that not all of the spectroscopic strength expected for these bands

is observed. Nevertheless, it seems likely that the observed transitions are due to fragmentation of the  $\frac{1}{2}^+[400]$  and perhaps the  $\frac{3}{2}^+[402]$  orbital, with the remaining spectroscopic strength probably distributed at excitation energies above those examined in the present experiment.

The close proximity of the  $l=0$  transition to the  $\frac{1}{2}^+[660]$  band in  ${}^{165}\text{Ho}$  raises the question of whether this fragmentation might be due to  $\Delta N=2$  mixing between the  $\frac{1}{2}^+[400]$  and  $\frac{1}{2}^+[660]$  orbitals. There is some evidence that  $\Delta N=2$  mixing is not the source of this fragmentation. If the  $l=0$  transition in  ${}^{165}\text{Ho}$  were due to a sizable  $\frac{1}{2}^+[400]$  component in the  $\frac{1}{2}^+$  member of the  $\frac{1}{2}^+[660]$  band, one would also expect appreciable mixing between the other members of the two bands. Yet the spectroscopic factor determined for the 1561-keV level indicates that essentially all the  $l=6$  strength is intact in one level. Moreover the similarity between the  $l=0$  and 2 spectroscopic factors in both isotopes, despite a downward shift in energy of some 200 keV in  ${}^{163}\text{Ho}$ , argues against mixing involving the  $\frac{1}{2}^+[660]$  orbital, which would be expected to rise in energy with decreasing deformation.

#### Comparison with theory

Along with the experimental values of  $U^2C_{ij}^2$  in Table III, the predictions of the Nilsson model are given in columns 5 and 9. The coefficients  $C_{ij}$  were extrapolated from Chi's tables<sup>19</sup> with the parameters  $\delta$ ,  $\kappa$ , and  $\mu$  set equal to 0.25, 0.50, and 0.65, respectively. The value of 0.25 for  $\delta$  corresponds to  $\beta_{20}=0.30$ , close to the value used in the coupled-channels scattering calculation. Since the hexadecapole moment is known<sup>12</sup> to be quite small at  $A \sim 165$ , it was set equal to zero in the calculation. The emptiness parameter  $U^2$  was calculated using the pairing force treated in the usual BCS approximation. The gap parameter  $\Delta$  was set equal to 850 keV, the value suggested by the even-odd mass differences. A survey by Ogle *et al.*<sup>23</sup> suggests that the chemical potential  $\lambda$  should be just below the ground state in the holmium isotopes. It was placed 100 keV below the ground state.

The theoretical predictions for  $U^2C_{ij}^2$  are significantly modified if the Coriolis coupling between particle motion and core rotation is included. This coupling introduces an additional term ( $H_{RPC}$ ) into the Hamiltonian which mixes all the single particle bands which originate in a given major oscillator shell. The basis used to diagonalize  $H_{RPC}$  should include all of these states. Unfortunately, only the energies of the bands nearest the ground state are known. Usually the energies

predicted by the Nilsson model are within about 0.5 MeV of experimentally observed energies. Consequently,  $H_{RPC}$  was first diagonalized in a basis in which the states whose energies are not known experimentally were placed at the energies predicted by the Nilsson model. The energy of each of these states was then moved up and down by 0.5 MeV to determine what effect this would have on the spectroscopic factors. All states predicted by the Nilsson model to be within 5 MeV of the ground state were included in the calculation. In many cases the presence of these additional states had a significant effect on spectroscopic factors of the low-lying states in the spectrum. However, in every case variation of  $\pm 0.5$  MeV in energies had almost no effect.

No systematic attempt was made to fit experimental energies by varying bandhead energies and moments of inertia. In cases where strong mixing occurred for bands near each other, small changes were made in bandhead energies to test the sensitivity of the predicted spectroscopic factors to the precise positions of these states. These small changes in bandhead energies had a significant effect on the spectroscopic factors for several members of the  $\frac{1}{2}^+[411]$  and  $\frac{3}{2}^+[411]$  bands. For these states, the initial excitation energies with no Coriolis interaction were adjusted so that the resulting excitation energies would be correct when Coriolis effects were included.

The results of this calculation are given in Table III, columns 6 and 10. The over-all agreement with the experimental strengths is somewhat improved. In particular one can understand why the  $\frac{3}{2}^+[411]$  bandhead is observed in  $^{163}\text{Ho}$  and not in  $^{165}\text{Ho}$ . However, the predicted spectroscopic factor for this state is still a factor of 4 smaller than the experimental value obtained for  $^{163}\text{Ho}$ .

#### V. CONCLUDING REMARKS

In general the qualitative agreement between the experimentally determined spectroscopic factors and the Coriolis-modified Nilsson-model predictions is fairly good, although there is a tendency on the average for the experimental values to be larger than the theoretical ones. In fact, the level-by-level comparison on an absolute basis would be somewhat improved if the experimental values were uniformly reduced by 30–40%. In particular this would bring better agreement for the  $\frac{5}{2}^+[402]$  bandhead in both nuclei, which is predicted to have a spectroscopic factor near unity, and for several members of the  $\frac{1}{2}^+[411]$ ,  $\frac{3}{2}^+[411]$ , and  $\frac{1}{2}^-[541]$  bands. Previous studies of proton-transfer reactions on rare-earth nuclei

have employed similar renormalizations, with the over-all normalization of the  $(^3\text{He}, d)$  reaction generally being treated as a free parameter. Since this normalization is not perfectly determined and parameter choices can introduce systematic biases into the predicted DWBA cross sections, some renormalization is not unreasonable. Moreover, we note that when  $(^3\text{He}, d)$  reactions at comparable bombarding energies on the lead isotopes are analyzed using our choice of potential parameters, roughly the same reduction would have to be applied to the resulting spectroscopic factors to bring them into agreement with shell-model expectations.<sup>9,18</sup> Thus, the results of the present experiment are in qualitative agreement not only with the relative strengths predicted by the Nilsson model but, if the  $(^3\text{He}, d)$  experiments on lead are taken as a "calibration", with the absolute strengths as well.

The evidence for significant contributions from two-step processes to the reaction, based on the present DWBA analysis, is necessarily indirect and at best inconclusive. The influence of these processes has been found to be rather important in neutron-transfer reactions at lower energies, and the large inelastic scattering cross sections measured for both  $^3\text{He}$  and deuteron projectiles suggest that they would be important here as well. Nonetheless, apart from the transition to the  $\frac{5}{2}^-$  member of the  $\frac{1}{2}^-[541]$  band in both  $^{165}\text{Ho}$  and  $^{163}\text{Ho}$  noted earlier, the measured  $(^3\text{He}, d)$  angular distributions are generally well-reproduced by the one-step DWBA, and while there are some discrepancies there is no obvious disruption of the distribution of strengths from what would be expected on the basis of the Nilsson model. However, preliminary coupled-channels calculations for the  $(^3\text{He}, d)$  reactions studied in this experiment indicate that indirect processes are indeed important for some transitions and that more realistic form factors are also necessary for an adequate description of the reaction. The generally good agreement obtained with the DWBA appears to be due to a tendency for these effects, when they are important, to roughly cancel each other. However, there is no guarantee that this is a universal effect. The investigation of these effects is near completion and will be reported in a forthcoming paper.

The authors are greatly indebted to K. T. Hecht for countless valuable discussions and for reading the manuscript prior to submission. The assistance of P. J. and A. D. Ellis in making the coupled-channels analysis of the scattering problem is gratefully acknowledged.

- \*Work supported in part by the U. S. Atomic Energy Commission.
- † Present address: School of Physics and Astronomy, The University of Minnesota, Minneapolis, Minnesota 55455.
- ‡ Present address: Physics Department, University of Indiana, Bloomington, Indiana 47401.
- <sup>1</sup>J. Ungrin, D. G. Burke, and M. W. Johns, Nucl. Phys. A132, 322 (1969); M. T. Lu and W. P. Alford, Phys. Rev. C 3, 1243 (1971); R. A. O'Neil, D. G. Burke, and W. P. Alford, Nucl. Phys. A167, 481 (1971); R. H. Price, D. G. Burke, and M. W. Johns, *ibid.* A176, 338 (1971); J. S. Boyno and J. R. Huizenga, Phys. Rev. C 6, 1411 (1972).
- <sup>2</sup>N. K. Glendenning and R. S. Mackintosh, Nucl. Phys. A168, 575 (1971); R. J. Ascuitto, C. H. King, and L. J. McVay, Phys. Rev. Lett. 29, 1106 (1972); C. H. King, R. J. Ascuitto, N. Stein, and B. Sorensen, *ibid.* 29, 71 (1972); H. Schulz, H. J. Wiebicke, and F. A. Gareev, Nucl. Phys. A180, 625 (1972); L. J. McVay, R. J. Ascuitto, and C. H. King, Phys. Lett. 43B, 119 (1973).
- <sup>3</sup>J. R. Comfort, unpublished.
- <sup>4</sup>L. Funke, K. H. Kaun, P. Kemnitz, H. Sodan, and G. Winter, Nucl. Phys. A190, 576 (1972).
- <sup>5</sup>G. Mauron, J. Kern, and O. Huber, Nucl. Phys. A181, 489 (1972).
- <sup>6</sup>G. R. Satchler, Ann. Phys. 3, 275 (1958).
- <sup>7</sup>W. T. Pinkston and G. R. Satchler, Nucl. Phys. 72, 641 (1965).
- <sup>8</sup>E. Rost, Phys. Rev. 154, 994 (1967).
- <sup>9</sup>W. C. Parkinson, D. L. Hendrie, H. H. Duhm, J. Mahoney, and J. Saudinos, Phys. Rev. 178, 1976 (1969).
- <sup>10</sup>F. Hintenberger, G. Mairle, U. Schmidt-Rohr, G. J. Wagner, and P. Turek, Nucl. Phys. A111, 265 (1968).
- <sup>11</sup>P. J. Ellis and A. D. Ellis, private communication.
- <sup>12</sup>D. L. Hendrie, N. K. Glendenning, B. G. Harvey, O. N. Jarvis, H. H. Duhm, J. Saudinos, and J. Mahoney, Phys. Lett. 26B, 127 (1968).
- <sup>13</sup>K. E. G. Löbner, M. Vetter, and V. Hönig, Nucl. Data A7, 495 (1970).
- <sup>14</sup>See for example G. R. Satchler, H. W. Broek, and J. L. Yntema, Phys. Lett. 16, 52 (1965); F. T. Baker and R. S. Tickle, *ibid.* 32B, 47 (1970); F. T. Baker and R. S. Tickle, Phys. Rev. C 5, 544 (1972).
- <sup>15</sup>R. H. Siemssen and J. R. Erskine, Phys. Rev. 146, 911 (1966); Phys. Rev. Lett. 19, 90 (1967).
- <sup>16</sup>P. D. Kunz, unpublished.
- <sup>17</sup>R. H. Bassel, Phys. Rev. 149, 791 (1966).
- <sup>18</sup>K. A. Erb and W. S. Gray, Phys. Rev. C 8, 347 (1973).
- <sup>19</sup>B. E. Chi, Nucl. Phys. 83, 87 (1966).
- <sup>20</sup>R. W. Gales, R. A. Warner, W. C. McHarris, and W. H. Kelly, Phys. Lett. 44B, 59 (1973).
- <sup>21</sup>R. M. Diamond, B. Elbek, and F. S. Stephens, Nucl. Phys. 43, 560 (1963).
- <sup>22</sup>V. G. Soloviev and P. Vogel, Nucl. Phys. A92, 449 (1967).
- <sup>23</sup>W. Ogle, S. Wahlborn, R. Piepenbring, and S. Fredricksson, Rev. Mod. Phys. 43, 424 (1971).